Protein Science (1999), *8*:854–865. Cambridge University Press. Printed in the USA.

De novo design of a monomeric three-stranded antiparallel β-sheet

EVA DE ALBA,[1] JORGE SANTORO, MANUEL RICO, AND M. ANGELES JIMÉNEZ

Instituto de Estructura de la Materia, Consejo Superior de Investigaciones Científicas, Serrano 119, 28006 Madrid, Spain

(RECEIVED October 7, 1998; ACCEPTED December 16, 1998)

Abstract

Here we describe the NMR conformational study of a 20-residue linear peptide designed to fold into a monomeric three-stranded antiparallel β-sheet in aqueous solution. Experimental and statistical data on amino acid β-turn and β-sheet propensities, cross-strand side-chain interactions, solubility criteria, and our previous experience with β-hairpins were considered for a rational selection of the peptide sequence. Sedimentation equilibrium measurements and NMR dilution experiments provide evidence that the peptide is monomeric. Analysis of ^{1}H and ^{13}C-NMR parameters of the peptide, in particular NOEs and chemical shifts, and comparison with data obtained for two 12-residue peptides encompassing the N- and C-segments of the designed sequence indicates that the 20-residue peptide folds into the expected conformation. Assuming a two-state model, the exchange kinetics between the β-sheet and the unfolded peptide molecules is in a suitable range to estimate the folding rate on the basis of the NMR linewidths of several resonances. The time constant for the coil-β-sheet transition is of the order of several microseconds in the designed peptide. Future designs based on this peptide system are expected to contribute greatly to our knowledge of the many factors involved in β-sheet formation and stability.

Keywords: β-sheet; chemical exchange; coil-β-sheet dynamics; NMR; peptide design; protein folding

Secondary structure elements are important context-free models to study protein stability, as well as for understanding protein folding initiation events. The classical approach to study the factors involved in secondary structure formation, in the absence of tertiary interactions, is peptide design followed by peptide conformational analysis (Baldwin, 1986; Wright et al., 1988; Dyson & Wright, 1993). This approach has been most successful in determining important aspects of α-helix formation and stability (Scholtz & Baldwin, 1992; Lyu et al., 1993; Zhou et al., 1993; Muñoz & Serrano, 1994a, 1994b; Baldwin, 1995). On the other hand, the design of peptides able to fold into β-hairpins or β-sheets has been much less satisfactory, mainly as a consequence of their high tendency to aggregate, and low solubility. Both disadvantages are due to the amphipathic character of the β-structure and to the high content of hydrophobic residues, the ones with highest β-sheet propensities. In spite of this, some linear peptides have recently been shown to fold into monomeric β-hairpins in aqueous solution (Blanco et al., 1998; Maynard et al., 1998; Smith & Regan, 1997) or alcohol-water mixtures (Cox et al., 1993; Blanco et al., 1994; Searle et al., 1996). Furthermore, the design and structure elucidation of model β-hairpins has demonstrated that the conformation of the turn plays a key role in directing β-hairpin structure (de Alba et al., 1996, 1997a; Haque & Gellman, 1997). In addition, one of these model peptides proved useful in identifying favorable and nonfavorable cross-strand side-chain interactions for β-hairpin formation, as well as highlighting the importance of turn conformation in directing β-hairpin twist, and thus β-hairpin stability (de Alba et al., 1997b). From a dynamic point of view, the main

Reprint requests to: M. Angeles Jiménez, Instituto de Estructura de la Materia, Consejo Superior de Investigaciones Científicas, Serrano 119, 28006 Madrid, Spain; e-mail: angeles@malika.iem.csic.es.

[1]Present address: Laboratory of Biophysical Chemistry, National Heart, Lung and Blood Institute, National Institute of Health, Bethesda, Maryland 20892.

Abbreviations: Δ, line width observed at half maximum intensity of the signal; Δ*, weighted average line width at half maximum intensity of the resonance lines of each conformational state; $\Delta\delta_{C\alpha}$, Cα conformational shift; $\delta_{C_\alpha}^{obs}$, observed ^{13}C chemical shift for the C_α carbon; $\delta_{C_\alpha}^{RC}$, ^{13}C chemical shift for the C_α carbon in random coil state; Δ_{rc}, line width at half maximum intensity of the resonance line of the random coil state; Δ_s, line width at half maximum intensity of the resonance line of the sheet state; υ_{rc}, chemical shift of the random coil state in Hertz; υ_s, chemical shift of the sheet state in Hertz; 1D, one-dimensional; 2D, two-dimensional; 3D, three-dimensional; COSY, homonuclear correlated spectroscopy; HPLC, high performance liquid chromatography; HSQC, heteronuclear single quantum coherence spectroscopy; k_f, folding rate constant; M_{av}, averaged molecular weight; M_{th}, theoretical molecular weight; NMR, nuclear magnetic resonance; NOE, nuclear Overhauser effect; NOESY, nuclear Overhauser enhancement spectroscopy; ppm, parts per million; P_{rc}, population of unstructured conformations; P_s, population of sheet conformations; RMSD, root-mean-square deviation; ROESY, rotating frame NOE spectroscopy; T_2, transverse relaxation time; TOCSY, total correlation spectroscopy; TSP, sodium [3-trimethylsilyl 2,2,3,3-^{2}H] propionate.

problem in the study of secondary structure formation is its extremely fast kinetics. Only recently, new experimental techniques have been put forward, which allow for the observation of protein folding events, including secondary structure formation, in a time scale from nanoseconds to microseconds (Eaton et al., 1997).

The determination of the factors governing secondary structure formation is central for the de novo design of proteins. Up until now, attempts to design all-β proteins have not been very successful. The main evidence about β-sheet formation in all the designed proteins (Yibing & Erickson, 1994; Martin et al., 1996; Smith & Regan, 1997) comes from CD data. More definite evidence for globular 3D structure, with well-packed side chains in the interior of the protein, such as that provided by NMR or X-ray diffraction, is lacking. Therefore, a better understanding of the factors involved in β-structure formation is still needed for de novo design.

Our successful design of β-hairpin forming peptides as models to study β-hairpin formation (Blanco et al., 1993; de Alba et al., 1995, 1996, 1997a, 1997b) prompted us to go one step further on the way toward the rational design of all-β proteins. As a structural motif, we selected an antiparallel three-stranded β-sheet, a target that has become the subject of great activity during the course of this investigation. Kortemme et al. (1998) have succeeded in designing a 20-residue linear peptide, which forms a high population of a three-stranded antiparallel β-sheet, by using a backbone template and an iterative hierarchical approach of database information, together with an algorithm of compatible side-chain rotamers. Schenck and Gellman (1998) have recently reported the design of a triple-stranded antiparallel β-sheet (21 residues), which incorporates D-Pro in the two turns. Sharman and Searle (1998) have described a 24-residue peptide, which cooperatively forms a β-sheet in the presence of methanol. Ilyna et al. (1997) have described a de novo designed 33-mer peptide, which folds as a compact β-sheet sandwich tetramer, whereas Doig (1997) has reported on a 23-residue peptide that contains N-methyl amino acids to prevent aggregation. Our model consists of a 20-natural amino acid linear peptide, whose sequence is based on our previous experience in the design of β-hairpins. The peptide forms a significant population of the expected monomeric three-stranded antiparallel β-sheet in aqueous solution. Assuming a two-state transition, it is possible to estimate the exchange rate between folded and unfolded states from the NMR line widths of several resonances. The estimated exchange rates in our peptide system are in agreement with those reported for the unique case in which the rate of β-hairpin formation has been experimentally estimated (Muñoz et al., 1997). This result highlights the utility of our model system. Future designs based on it may help to identify key aspects of β-sheet folding.

Results

Peptide design

The simplest β-sheet structure that can be formed by a short linear peptide is a three stranded antiparallel β-sheet with turns linking the first and second strands, and the second strand to the third strand. We have designed a peptide able to form this motif keeping its length as short as possible, while allowing the strands to be long enough to accommodate the cross-strand hydrogen bonds and side-chain interactions needed to stabilize the structure. On the basis of these criteria, the β-sheet schematically represented in Figure 1A was adopted as the design target. The design contains two two-residue turns and three strands. The peptide sequence was selected taking into account experimental and statistical data on amino acid β-turn and β-sheet propensities, cross-strand side-chain interactions, solubility criteria, and our previous experience with β-hairpins. Repetition

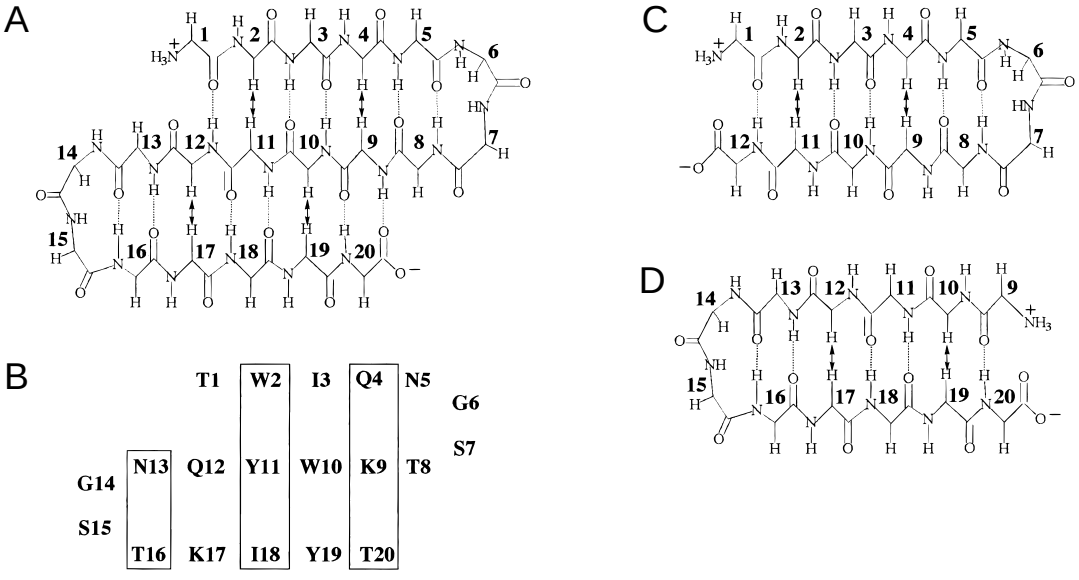

Fig. 1. A: Backbone schematic representation of the β-sheet model. Dotted lines indicate hydrogen bonds, and black arrows connect CαH protons that give rise to NOEs. A pair of facing residues is in a hydrogen bonded site when their CO and NH are hydrogen bonded, for example, pairs 3–10, 9–20, and 11–18. When their CO and NH are not hydrogen bonded, the pair of facing residues belongs to a nonhydrogen bonded site, for example, pairs 2–11, 4–9, 10–19, and 12–17. **B:** Sequence of peptide 1. Amino acids are located in their respective positions in the β-sheet represented in **A**. Amino acids located on the same side of the β-sheet plane are boxed. **C**, **D:** Backbone schematic representations of the β-hairpin structures adopted by peptides 2 and 3, respectively.

of residues was kept to a minimum to reduce possible NMR signal overlap. An optimal choice of turn residues is crucial (de Alba et al., 1996, 1997a, 1997b; Haque & Gellman, 1997). Type I′ and type II′ turns (Sibanda & Thornton, 1985) are the most frequently found in β-hairpin structures. The former suits the β-hairpin conformation better than the later due to their right-handed topology (Clothia, 1973). In contrast, type II′ turns are more planar (Sibanda & Thornton, 1985), which allows better backbone interstrand hydrogen bonding (Mattos et al., 1994). For our design, type II′ turns were chosen over type I′ turns because we anticipated that our β-sheet model, being small, will most probably need the most stable hydrogen bonding network possible. Turn residues G6,S7 and G14,S15 (Fig. 1B) were selected according to their high statistical probabilities to be at positions $i + 1$ and $i + 2$, respectively, in type II′ turns (Hutchinson & Thornton, 1994) and the preceding and following residues to the GS pair (N5,T8 and N13,T16) because present experimental evidence indicates that the interaction between the side chains of N and T is favorable for β-hairpin formation (de Alba et al., 1997a). It must be noted that residues N and G also have a high statistical probability to be at positions $i + 1$ and $i + 2$, respectively, of a type I′ turn (Hutchinson & Thornton, 1994) and that a designed 10-residue peptide with sequence YNGK at the turn region forms two different β-hairpins: one with a type I′ turn (YNGK) and the other with a type II′ turn (NGKT) (de Alba et al., 1997a). In the three-stranded β-sheet target peptide, undesirable type I′ turns could form with N5G6 and N13G14 at their preferred positions in a type I′ turn (Hutchinson & Thornton, 1994). To avoid the formation of this type of turn, amino acid Q, an unfavorable residue at position *i* of a type I′ turn, was chosen for residues 4 and 12 (Hutchinson & Thornton, 1994). For the same reason, we included S at the $i + 2$ position of the type II′ turns (residues 7 and 15) instead of the statistically more favorable N. This change has the additional advantage of not repeating N, already present at positions 5 and 13.

While the presence of charged residues was considered necessary to increase solubility and prevent aggregation, these residues have low β-sheet propensities. Therefore, only two charged residues were introduced. Positively charged residues were preferred since they remain in the charged state over broader pH ranges for use in NMR. Lysine was selected as it lends good solubility to β-hairpin forming peptides (Ramírez-Alvarado et al., 1996; de Alba et al., 1997a). To avoid the formation of an amphipathic β-sheet that could cause aggregation, the charged residues were designed to point to opposite sides of the sheet plane and to be far from each other, distributing the charge as much as possible. At least one charged residue should be located in the middle strand, which is the most protected from solvent, to promote its solvation. Positions 9 and 17 satisfied the previously mentioned conditions and contribute to the distribution of the four charges, C- and N-termini plus the two K residues, throughout the sheet.

Good β-sheet formers, such as I, Y, W, and T, were selected for the eight remaining positions (Chou & Fasman, 1974; Kim & Berg, 1993; Minor & Kim, 1994a, 1994b; Smith et al., 1994; Muñoz & Serrano, 1994b; Swindells et al., 1995). These residues were distributed to avoid a marked amphipathicity. The more hydrophobic residues I, Y, and W were placed at positions 2, 11, and 18 as well as in 3, 10, and 19, whereas T was placed at the N- and C-termini. The packing of the hydrophobic residues was based on statistical results of cross-strand side-chain interactions, which indicate favorable interactions between pairs I-W and I-Y in hydrogen bonded sites of antiparallel β-sheets and between the pair Y-W in nonhydrogen bonded sites (Wouters & Curmi, 1995). The designed sequence (Fig. 1A,B) contains the pairs W2–Y11 and W10–Y19 in nonhydrogen bonded sites and the pairs I3–W10 and Y11–I18 in hydrogen bonded sites. Other β-sheet forming residues, such as V or F, could have been selected but statistical pair correlations V-Y and V-W are not as favorable as I-Y and I-W (Wouters & Curmi, 1995); F, which may form favorable interactions with Y and W in hydrogen bonded sites (Wouters & Curmi, 1995), is an aromatic residue that could produce resonance overlap with Y and W.

The designed peptide is a monomer

Since most β-sheet forming peptides have a strong tendency to aggregate, it is imperative to confirm that the designed peptide 1 is monomeric under the conditions required for NMR. To this end, sedimentation equilibrium experiments were performed at 0.1 and 1 mM peptide concentrations in aqueous solution. Average molecular weights obtained for these concentrations were significantly lower than the molecular weight calculated from the amino acid composition. This is a typical result in sedimentation equilibrium of nonideal samples, where the presence of repulsive electrostatic interactions between peptide charges opposes ultracentrifuge force (McRorie & Voelker, 1993; Ralston, 1993). To circumvent this problem, 150 mM NaCl was added. In the 1 mM solution, peptide 1 precipitated at this high ionic strength as well as at micromolar concentrations of NaCl. However, the 0.1 mM sample had no solubility problems upon salt addition. Sedimentation equilibrium measurements on the 0.1 mM sample at 150 mM NaCl gave an average molecular weight (M_{av}) very close to the one calculated from the residue composition (M_{th}), thus indicating a monomeric state of the peptide (Fig. 2A,B), $M_{av}/M_{th} = 1.03 \pm 0.05$). To ensure that the peptide was a monomer up to 1 mM, 1D ^{1}H-NMR spectra were recorded for the 0.1 and 1 mM peptide samples. The absence of changes in either line widths or chemical shifts between the spectra of the concentrated and diluted samples (Fig. 2C,D) is very good evidence that the peptide is monomeric at 1 mM concentration.

The designed peptide forms the target three-stranded antiparallel β-sheet

The intensities of nuclear Overhauser enhancement (NOE) cross-correlations are a function of interproton distances and they provide the most relevant NMR structural information. The NOEs characteristic of antiparallel β-sheet are those involving CαH*i*–CαH *j*, CαH*i*–NH $j + 1$, and NH$i + 1$–NH $j - 1$ protons, where *i* and *j* are residues that face each other in adjacent β-strands, with the CαH protons pointing toward the interior of the sheet. The shortest distance and correspondingly the most intense NOEs are those between the CαH*i*–CαH *j* protons. They are the main diagnostic of the formation of the β-sheet (Wüthrich et al., 1984; Wüthrich, 1986). The relatively strong CαH–CαH NOEs between residues W2–Y11, Q4–K9, Q12–K17, and W10–Y19, unambiguously identified in the NOESY spectrum of the designed peptide (Fig. 3), are those expected for our target β-sheet (Fig. 1A). Some other observed NOEs (Table 1) are further evidence that peptide 1 populates the expected β-sheet structure, such as those between $i, i + 2$ residues in the same strand involving protons in either the side chains or the main chain, as well as those between *i* and *j* side-chain protons of cross-strand residues. The severe overlap of

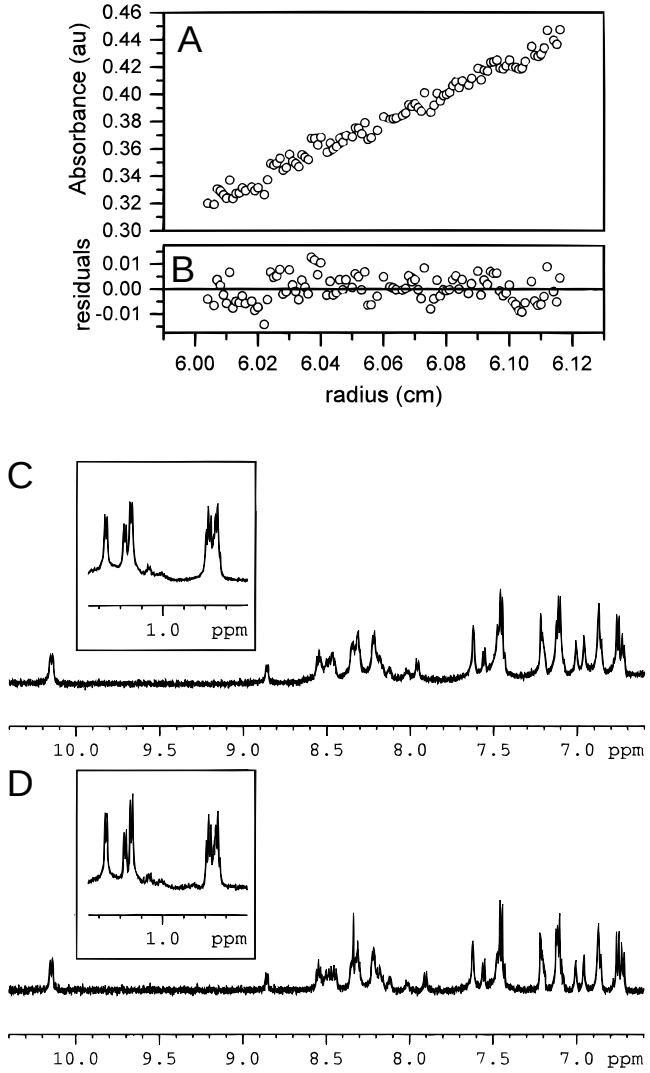

Fig. 2. (**A**) Peptide absorbance vs. centrifuge radius for a designed peptide 1 sample at 0.1 mM, pH 3.4, 10 °C. (**B**) Residuals of the fit of the data in **A** to the relation $\ln Cr^2$ (C denotes concentration, r radius). 1D ^{1}H NMR spectra of the designed peptide 1 (10 °C, pH 3.4) at (**C**) 1 mM and (**D**) 0.1 mM.

the NH resonances precludes the observation of many of the expected NH–NH interstrand NOEs.

The compatibility of the observed NOEs with the β-sheet target can be checked by calculating a structure on the basis of distance constraints derived from the intensities of all unambiguously assigned medium- and long-range NOEs (Table 1). Signal overlap, originated by the repetitive sequence of the peptide, precludes the unambiguous assignment of many medium- and long-range NOEs. In spite of that, it is still possible to calculate a structure on the basis of observed NOEs. As a consequence of the small number of restraints used in the calculation (20 distance constraints; Table 1), the calculated structures (see Materials and methods) are not well defined. However, the superposition of the backbone atoms of 10 calculated structures (Fig. 4) helps to visualize the series of conformations that satisfies the experimental constraints, and confirms the compatibility of the observed NOEs with the three-stranded antiparallel target β-sheet.

Table 1. *Medium- and long-range NOE connectivities of the designed peptide 1 (1 mM of peptide in aqueous solution, pH 3.4, 10 °C)*

^{1}H resonance in		
Residue *i*	Residue *j*	NOE intensity[a]
Cα H T1	CγH_3 and/or CδH_3 I3[b]	m-s
Cβ H T1	CγH_3 and/or CδH_3 I3[b]	m-s
Cα H T1	Cε$_3$H Y11	w
Cββ′H W2	Cε$_3$H W10	vw
Cα H W2	Cα H Y11	m-s
Cε$_3$H W2	Cα H Y11	w
Cε$_3$H W2	Cβ′H N13	w
Cα H Q4	Cα H K9	s
CγH_3 and/or CδH_3 I3[b]	Cα H N5	m
CγH_3 and/or CδH_3 I3[b]	NH N5	w
CγH_3 and/or CδH_3 I3[b]	Cε$_3$H W10	w
CγH_3 and/or CδH_3 I3[b]	Cδ1H W10	w-m
Cδ1H W10	Cβ′H Q12	w
Cα H W10	Cα H Y19	m-s
Cδ H Y11	Cα H N13	w
Cδ H Y11	Cγ′H I18	vw
Cδ H Y11	Cγ H I18	w
Cδ H Y11	CγH_3 I18	m
Cε H Y11	Cα H N13	m
Cε H Y11	Cβ′H N13	m
Cε H Y11	CγH_3 I18	m
Cε H Y11	Cδδ′H K9	w
Cα H Q12	Cα H K17	m-s
NH T16	Cα′H G14	m
Cββ′H K17	Cε H Y19	m
NH T20	CγH_3 I18	vw

[a] The intensity of the NOEs are classified as: s, strong; m, medium; m-s, intermediate between strong and medium; w, weak; w-m, intermediate between weak and medium; vw, very weak.

[b] Because of their ambiguity these NOEs were not included in the structure calculation.

Since there are no established methods to quantify the amount of β-structure formed by peptides (de Alba et al., 1996, 1997a; Ramírez-Alvarado et al., 1997; Blanco et al., 1998), we have used the intensity of the Cα H*i*–Cα H *j* NOEs to obtain an estimate. The intensity of the NOE between the Cβ H protons of residue Y19, two protons with a known and fixed distance, was used as a reference. The Cα H*i*–Cα H *j* distance expected for a fully populated β-sheet was taken as the averaged Cα H*i*–Cα H *j* distance found for antiparallel β-sheets in proteins (Wüthrich, 1986). This is the same procedure used previously for β-hairpin forming peptides (de Alba et al., 1996, 1997a; Blanco et al., 1998; Maynard et al., 1998; Smith & Regan, 1998). Apart from the experimental error in the NOE intensity measurement, error sources for this method arise from the potential existence of different local correlation times along the peptide chain, and/or between the folded and unfolded peptide, and small variations in the actual Cα H*i*–Cα H *j* distance with respect to the averaged value in antiparallel β-sheets taken as reference. Table 2 summarizes the β-structure percent populations obtained from each Cα H*i*–Cα H *j* NOE observed for the designed peptide 1 at 10 °C. On the basis of these calculations, the β-sheet population is 13–31% at this temperature.

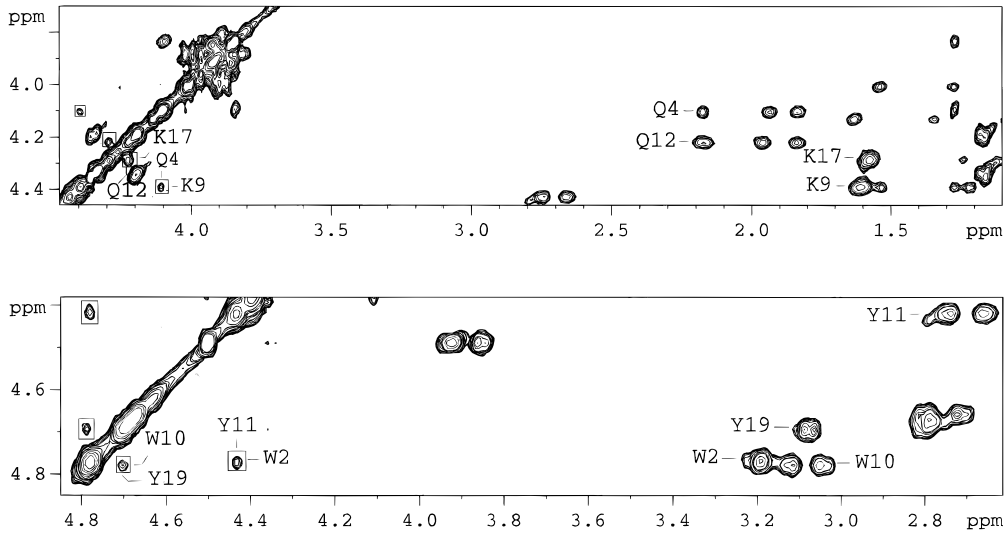

Fig. 3. Regions of NOESY spectrum of the 20-residue designed peptide 1 at 10 °C, pH 3.4, D_2O, 1 mM, showing the CαH–CαH NOEs characteristic of the β-sheet represented in Figure 1A.

Conformational chemical shifts of CαH protons are often used to delineate and quantitate secondary structure populations. However, our designed peptide contains multiple aromatic amino acids, which normally introduce large ring current shifts obscuring the observation of true secondary structure conformational shifts. The ^{13}C shifts are not so dependent on field effects as ^{1}H shifts, and are also related with secondary structure (Spera & Bax, 1991). In particular, C_α conformational chemical shifts are recognized as the most useful and sensitive parameter to detect and identify secondary structure (Buckley et al., 1993; Gronenborn & Clore, 1994; Yao et al., 1997; Guerois et al., 1998). The pattern of $\Delta\delta_{C_\alpha}$ conformational shifts ($\Delta\delta_{C_\alpha} \equiv \delta_{C_\alpha}^{obs} - \delta_{C_\alpha}^{RC}$, where $\delta_{C_\alpha}^{RC}$ are the δ-values of the random coil (Wishart et al., 1995)) of the designed peptide 1 (Fig. 5) is the pattern expected for a three-stranded β-sheet: large negative shifts for C_α carbons in the strands and null or slightly positive shifts in the turns (Spera & Bax, 1991). A rough estimation of the population of β-sheet and β-hairpin, assuming $\Delta\delta_{C_\alpha}$ (100% β) = −1.48 ppm (Spera & Bax, 1991), provides values in the range 30–55%, depending on the signals selected for the estimation.

The NMR data obtained here are compatible with the presence of a single structured form, the three-stranded antiparallel β-sheet, in equilibrium with the random coil. However, linear peptides in solution commonly exist as conformational ensembles of interconverting structures in fast exchange on the NMR time scale. NOESY spectra of linear peptides then contain NOE cross peaks representative of all populated conformations. Therefore, it is possible that the independent formation of the two hairpins embodied in the β-sheet could give the same NOE pattern as the complete three-stranded structure. Only in the case of 100% population for each β-hairpin, as evaluated from the corresponding NOEs, could we confirm the existence of a 100% population of the entire β-sheet.

Other NMR parameters allow us to discriminate between the presence of the three-stranded antiparallel β-sheet in equilibrium with the random coil, and the existence of an equilibrium between four states: the three-stranded antiparallel β-sheet, two states in which the only structured part is the two constituent β-hairpins, and the random coil. Since $^{13}C_\alpha$ chemical shifts are dominated by ϕ,ψ torsion angles with only minor corrections arising from hydrogen bonding and charge electrostatic effects (de Dios et al., 1993), the $\Delta\delta_{C_\alpha}$ conformational shifts should be similar in the central and in the external strands of the three-stranded β-sheet. In contrast, if the peptide were forming exclusively the two hairpins in about equal populations, the $\Delta\delta_{C_\alpha}$ conformational shifts should

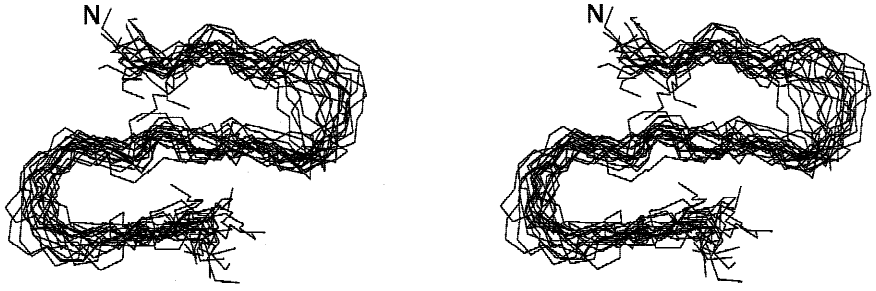

Fig. 4. Backbone superposition of 10 calculated structures of the designed peptide 1. Root-mean-square deviations for the superposition of 20 calculated structures, which showed the lowest values of the target function and did not violate the experimental constraints in more that 0.2 Å, are 2.3 ± 0.5 Å for backbone atoms and 3.2 ± 0.5 Å for all heavy atoms.

Table 2. *Estimation of the population of β-structure formed by peptides 1, 2, and 3 in D_2O at pH 3.25 and 10 °C from the CαH-CαH NOE intensity*

	Population of β-structure (%) in		
CαH–CαH NOE	Designed peptide 1	Peptide 2	Peptide 3
W2–Y11	24	17	—
Q4–K9	31	14	—
Q12–K17	19	—	18
W10–Y19	13	—	15

be twice as large in the common strand than in the edge strands. The fact that the $\Delta\delta_{C_\alpha}$ conformational shifts are about equal in all three strands (Fig. 5) is in favor of the presence of the entire three-stranded β-sheet.

The temperature dependence of the δ-values of peptide 1's nonexchangeable protons was followed by a series of 1D and 2D TOCSY spectra in the range 5–80 °C. Some of them present a large Δδ between low and high temperatures (in particular, Y11 C_δH protons show a Δδ of 0.12 ppm), but the temperature dependence appears to be monotonously linear, suggesting a broad transition between structured and unfolded states (data not shown). Nevertheless, it is worthwhile to note that the protons whose δ-values show the largest temperature dependence are those having the largest δ deviations from the random coil values at low temperature. At high temperature, their δ-values approach those of the random coil. This is the behavior expected for a peptide that adopts a structure at low temperature that unfolds at high temperature.

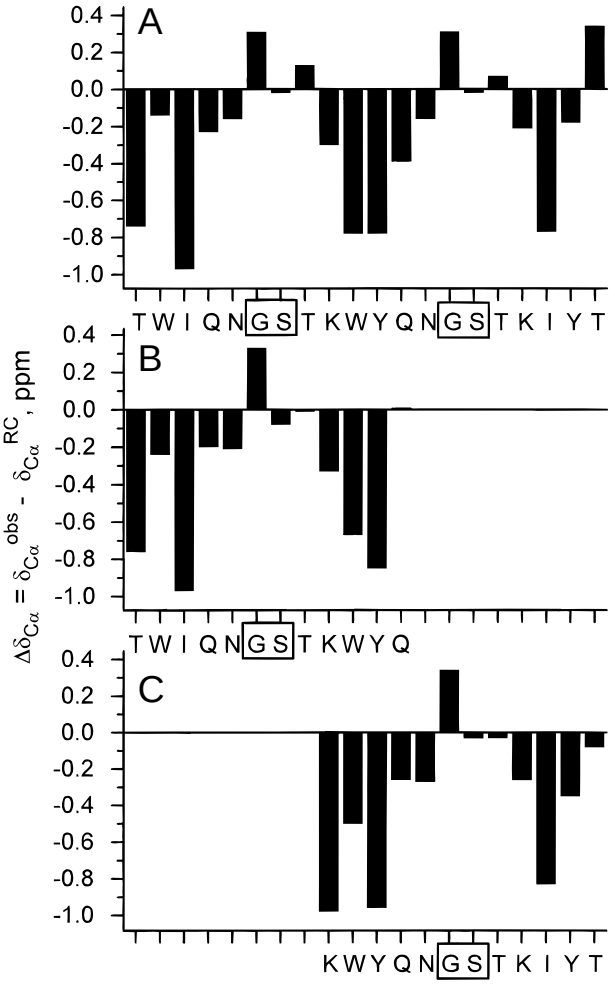

Fig. 5. Conformational shifts of the Cα carbons for the 20-residues designed (**A**) peptide 1 and for (**B**) peptide 2 and (**C**) peptide 3 as a function of sequence. Turn residues are boxed.

To further confirm the formation of the three-stranded β-sheet as well as to detect the existence of any positive cooperativity, the conformational properties of two shorter peptides encompassing the single β-hairpins were examined by NMR. They were peptide 2 (TWIQNGSTKWYQ) and peptide 3 (KWYQNGSTKIYT), corresponding to residues 1–12 and 9–20, respectively, of the designed peptide. Assignments for peptides 2 and 3 are given in Table 3. The fact that 1D ^{1}H-NMR spectra recorded for 2 and 0.1 mM samples of peptides 2 and 3 showed no change, within experimental error, in either chemical shifts or line widths, indicates that both peptides are monomeric (data not shown). The sets of NOEs observed for these peptides (see Supplementary material in Electronic Appendix; Tables SM1,2), which include CαH–CαH NOEs between residues W2–Y11 and Q4–K9 in peptide 2 and between residues Q12–K17 and W10–Y19 in peptide 3, indicate that both of them form the expected 2:2 β-hairpins with type II′ turns, involving the residues NGST (see Fig. 1C,D). The profile of $\Delta\delta_{C_\alpha}$ conformational shifts of peptides 2 and 3 (Fig. 5) with large negative shifts in the strands and null or slightly positive shifts in the turns (Spera & Bax, 1991), additionally confirm the formation of β-hairpins by both peptides. Population of β-hairpin in peptide 2 is slightly smaller (as estimated from the CαH–CαH NOEs; Table 2), or approximately the same (as estimated from the $\Delta\delta_{C_\alpha}$ conformational shifts in the β-strands; Fig. 5) as the one formed in peptide 1, whereas the population of the β-hairpin in peptide 3 (as estimated by either of the two methods; Table 2, Fig. 5) roughly corresponds to the population in peptide 1. Therefore, the cooperativity, if any, must be very low.

A comparison of δ-values of nonexchangeable protons in nonterminal residues of peptides 1, 2, and 3 shows that in general they coincide within experimental error. However, there are some protons clustered around residues W10 and Y11, belonging to the central strand of the β-sheet, which show some discrepancies. In the longer peptide, if we have a mixture of the two β-hairpins, the observed shifts should be a population weighted average of those observed in the shorter peptides 2 and 3. This is not so for protons Cβ′H, Cε3H, and Cδ1H of W10, and CβH of Y11 (see Table 3), suggesting that these protons may feel a distinct local magnetic environment in the longer peptide, which could correspond to the three-stranded β-sheet. This observation provides further support that the designed peptide 1 adopts the entire β-sheet conformation.

Estimation of random coil–β-sheet transition rate constants

Proton resonances of the designed peptide 1 undergo a large and selective broadening when decreasing the temperature (Fig. 6). NMR line widths depend inversely on the transverse relaxation time T_2 (Mooney, 1971a), which in turn depends on the molecular motion (Freeman, 1988a). At low temperatures molecular motion slows down and T_2 decreases, giving rise to larger NMR line

Table 3. *Chemical shifts of peptides 1, 2 and 3 in aqueous solution (pH 3.4 and 10 °C)*[a]

Residue	Proton	δ (ppm) in peptide 1	2	3
T1	CαH	3.84	3.82	
	CβH	4.10	4.09	
	$C\gamma H_3$	1.28	1.26	
W2	NH	8.90	8.88	
	CαH	4.77	4.78	
	CβH	3.20, 3.20	3.19, 3.19	
	$C\delta_1H$	7.22	7.22	
	$N\epsilon_1H$	10.16	10.16	
	$C\epsilon_3H$	7.56	7.55	
	$C\zeta_2H$	7.46	7.46	
	$C\zeta_3H$	7.12	7.12	
	$C\eta_2H$	7.22	7.22	
I3	NH	8.21	8.21	
	CαH	4.01	4.01	
	CβH	1.56	1.56	
	CγH	1.30, 1.01	1.29, 1.01	
	$C\gamma H_3$	0.75	0.74	
	$C\gamma H_3$	0.75	0.74	
Q4	NH	8.34	8.35	
	CαH	4.11	4.17	
	CβH	1.94, 1.85	1.96, 1.86	
	CγH	2.19, 2.19	2.22, 2.22	
	NεH	7.51, 6.90	7.52, 6.90	
N5	NH	8.60	8.59	
	CαH	4.68	4.70	
	CβH	2.79, 2.79	2.82, 2.77	
	NδH	7.66, 6.99	7.66, 6.99	
G6	NH	8.58	8.60	
	CαH	3.97, 3.92	4.00, 3.91	
S7	NH	8.39	8.39	
	CαH	4.51	4.51	
	CβH	3.93, 3.86	3.94, 3.86	
T8	NH	8.26	8.25	
	CαH	4.35	4.34	
	CβH	4.20	4.17	
	$C\gamma H_3$	1.16	1.14	
K9	NH	8.35	8.35	
	CαH	4.37	4.38	3.95
	CβH	1.61, 1.61	1.58, 1.58	1.80, 1.80
	CγH	1.26, 1.22	1.22, 1.22	1.28, 1.28
	CδH	1.55, 1.55	1.53, 1.53	1.63, 1.63
	CεH	2.84, 2.84	2.82, 2.82	2.91, 2.91
	NζH	7.51	7.48	7.59
W10	NH	8.16	8.26	8.65
	CαH	4.75	4.64	4.81
	CβH	3.13, 3.05	3.17, 3.11	3.12, 3.12
	$C\delta_1H$	7.13	7.14	7.22
	$N\epsilon_1H$	10.18	10.16	10.18
	$C\epsilon_3H$	7.43	7.48	7.50
	$C\zeta_2H$	7.46	7.46	7.47
	$C\zeta_3H$	7.09	7.12	7.12
	$C\eta_2H$	7.21	7.22	7.23
Y11	NH	8.06	7.85	8.19
	CαH	4.42	4.40	4.42
	CβH	2.75, 2.68	2.77, 2.63	2.84, 2.75
	CδH	6.87	6.84	7.00
	CεH	6.73	6.73	6.74
Q12	NH	8.26	7.89	8.31
	CαH	4.20	4.07	4.13
	CβH	1.96, 1.85	1.99, 1.83	1.98, 1.90
	CγH	2.18, 2.18	2.16, 2.16	2.23, 2.23
	NεH	7.49, 6.90	7.52, 6.89	7.56, 6.94
N13	NH	8.52		8.57
	CαH	4.66		4.70
	CβH	2.82, 2.74		2.84, 2.75
	NδH	7.65, 7.04		7.66, 7.04
G14	NH	8.54		8.60
	CαH	4.01, 3.90		4.02, 3.92
S15	NH	8.39		8.44
	CαH	4.51		4.52
	CβH	3.93, 3.86		3.94, 3.88
T16	NH	8.26		8.24
	CαH	4.34		4.35
	CβH	4.20		4.21
	$C\gamma H_3$	1.19		1.19
K17	NH	8.36		8.38
	CαH	4.28		4.33
	CβH	1.59, 1.59		1.61, 1.61
	CγH	1.24, 1.12		1.26, 1.14
	CδH	1.50, 1.45		1.51, 1.46
	CεH	2.76, 2.76		2.76, 2.76
	NζH	7.45		7.46
I18	NH	8.24		8.28
	CαH	4.14		4.16
	CβH	1.65		1.66
	CγH	1.35, 1.08		1.36, 1.09
	$C\gamma H_3$	0.80		0.81
	$C\delta H_3$	0.78		0.80
Y19	NH	8.52		8.55
	CαH	4.70		4.71
	CβH	3.10, 2.82		3.06, 2.74
	CδH	7.11, 7.11		7.05, 7.05
	CεH	6.76, 6.76		6.75, 6.75
T20	NH	8.00		8.04
	CαH	4.27		4.30
	CβH	4.27		4.30
	$C\gamma H_3$	1.16		1.16

[a] The underscored values correspond to those protons whose δ values in peptide 1, and in either peptide 2 or 3, differ more than 0.05 ppm, excluding K9 and Q12 protons and all NH protons.

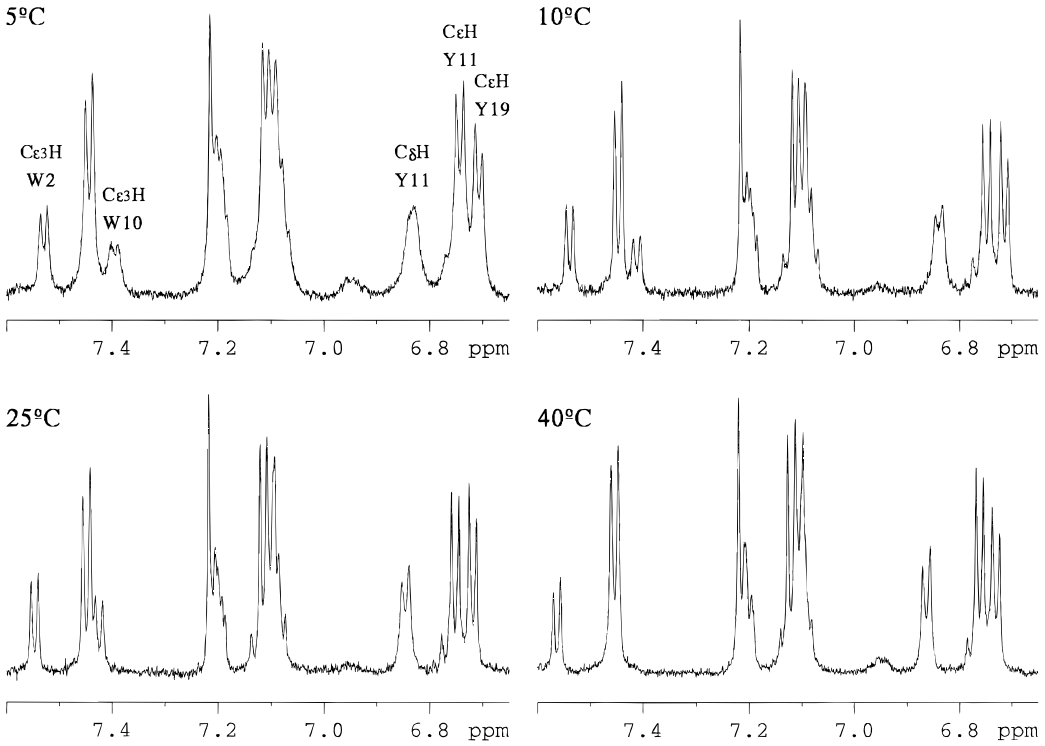

Fig. 6. 1D ^{1}H NMR spectra of the designed peptide 1 (1 mM, pH 3.4, D_2O) at 5, 10, 25, and 40 °C. The resonances used to estimate coil–β-sheet transition rate constants are indicated at the 5 °C spectrum.

widths. The observed NMR signal broadening cannot be explained by that common effect, since it is larger than the one usually observed in peptides of the same size, and it is not homogeneously distributed along the peptide sequence. Some resonances of residues W10 and Y11, both located in the middle strand (Fig. 1), are much broader than the rest. Peptide aggregation can be discarded as the origin of line broadening, once the monomeric state of the peptide has been demonstrated. Assuming a two-state model for the random coil-β-sheet transition, the absence of a set of resonances for each state indicates that exchange is fast, but the unusually large line width at low temperature suggests that the equilibrium is approaching the intermediate exchange region, making it possible to estimate the rate constant for the formation of the β-sheet. To estimate the rate, we used the nonoverlapping signals at the 1D ^{1}H-NMR spectra of peptide 1 in aqueous solution at pH 3.4, 10 °C and 5 °C. These signals belong to the CϵH proton of residue W2, located in the N-terminal strand; the CϵH proton of W10, and the CδH and CϵH protons of Y11, from the middle strand; as well as the CϵH proton of Y19, which lies in the C-terminal strand. Other resonances could not be used because of signal overlap, and in the case of the NH resonances, because they exchange with solvent and lack appropriate random coil chemical shift values.

A general equation for estimating the rate of β-sheet formation (Mooney, 1971b) is

$$k_f = [P_{rc}P_s^2 4\pi(\upsilon_{rc} - \upsilon_s)^2]/(\Delta - \Delta^*) \quad (1)$$

where P_{rc} and P_s denote the populations of the unstructured and sheet conformations, respectively; $(\upsilon_{rc} - \upsilon_s)$ is the chemical shift difference, in Hertz, between the two conformational states for the same proton; Δ is the line width observed at half maximum intensity; and Δ* is the weighted average line width at half maximum intensity of the resonance lines of each conformational state (Δ_{rc} and Δ_s for the random coil and the sheet states, respectively), $\Delta^* = P_{rc}\Delta_{rc} + P_s\Delta_s$.

Values for υ_{rc}, υ_s, Δ_{rc}, and Δ_s cannot be obtained directly from the NMR spectra of peptide 1. The υ_{rc} was taken as the chemical shift values in unstructured tetrapeptides (Bundi & Wüthrich, 1979). The Δ_{rc} can be estimated from the resonances at high temperature (40 °C), where exchange rate constants are very fast relative to the NMR time scale and the broadening caused by chemical exchange is negligible (Freeman, 1988b). We used 13% (lower limit from NOE data; Table 2) and 55% (from $^{13}C_\alpha$ shifts) as the lower and upper limits of β-sheet structure population to estimate υ_s (the observed chemical shift is the weighted average of the random coil and sheet chemical shifts). As a lower limit of the also unknown Δ*, we assumed that the line width of a resonance in the sheet conformation is the same as that observed in the coil state. Thus, $\Delta^*_{\min} = \Delta_{rc}$.

On the basis of these assumptions, we have estimated the coil-sheet transition rate constants given in Table 4 at 10 °C. The upper limit for the time required by the coil state to fold into the β-sheet ranges from 16–45 μs at 5 °C and 4–14 μs at 10 °C. The values obtained from different resonances are consistent. The errors in these values can be rather large since many assumptions have been made, but we think that these rates are indicative of the time range of β-sheet folding.

Discussion

We have shown from a careful analysis of ^{1}H and ^{13}C-NMR parameters that the designed 20-residue peptide 1 is able to form the target three-stranded antiparallel β-sheet in aqueous solution.

Table 4. *Estimation of average residence times of resonances in the coil state at 10 °C*

Resonance	Δ_{obs}[a] (Hz)	Δ_{rc}[b] (Hz)	δ_{obs}[a] (ppm)	δ_{rc}[c] (ppm)	δ_s[d] (ppm) at population of 13%	δ_s[d] (ppm) at population of 55%	$\tau_{max} = 1/k_f$ (μs) at population of 13%	$\tau_{max} = 1/k_f$ (μs) at population of 55%
CεH Y11	3.10	2.77	6.71	6.86	5.71	6.59	4	7
CδH Y11	7.08	3.65	6.84	7.15	4.77	6.59	9	18
CεH Y19	3.10	2.77	6.75	6.86	6.01	6.66	7	13
Cε3H W10	5.31	3.98	7.41	7.65	5.80	7.21	6	11
Cε3H W2	3.98	3.32	7.54	7.65	6.80	7.45	14	27

[a] Values taken from peptide 1 1D ^{1}H NMR spectrum in D_2O, pH 3.25, and 10 °C.
[b] Values taken from peptide 1 1D ^{1}H NMR spectrum in D_2O, pH 3.25 and 40 °C.
[c] Values taken from Wüthrich (1986).
[d] Chemical shift of the corresponding proton in the β-sheet conformation.

Considering that β-turn sequence has been shown to determine the alignment of strands in β-hairpin formation (de Alba et al., 1996, 1997a, 1997b; Haque & Gellman, 1997), the choice of a β-turn sequence suitable to adopt a β-hairpin 2:2 and unable to form any other shifted turn has probably been at the root of the success of our β-sheet design. This type of turn favors the right alignment of backbone atoms in the β-strands for the formation of the hydrogen bonding network as well as to approach the facing side chains so that they can interact and contribute to the stability of the final β-sheet.

An important point to be discussed concerns whether the formation of the three-stranded antiparallel β-sheet is cooperative, i.e., whether the formation of one of the hairpins promotes the collapse of the other. A comparison of the $^{13}C_\alpha$ chemical shifts of peptides 1, 2, and 3 led us to conclude that there was no sign of cooperativity in the formation of the three-stranded β-sheet. However, peptides 2 and 3 have end charges in their corresponding hairpins (Fig. 1C,D), whose interaction may contribute to increase the population of the individual hairpins. Such an electrostatic interaction has been shown to contribute to the stability of a nine-residue β-hairpin forming peptide (de Alba et al., 1995), and is absent in the three-stranded β-sheet (Fig. 1A). Accordingly, the formation of the β-sheet would show some degree of cooperativity, whose magnitude could be evaluated from the effect of the charge electrostatic interaction on the populations of the individual hairpins.

The question of whether β-sheet formation displays a cooperative behavior has been addressed in previous reports on designed short peptides able to form three-stranded antiparallel β-sheets. The 20-amino acid peptide designed by Kortemme et al. (1998) forms a high population of β-sheet and exhibits a cooperative behavior as deduced from a broad thermal transition. A broad sigmoidal melting curve is also observed for the 24-residue peptide designed by Sharman and Searle (1998), which folds into a three-stranded β-sheet in aqueous methanol. The linear temperature dependence of the Y11 C_δH chemical shift of our designed peptide 1 can be interpreted as a broader transition than that of the above peptide, corresponding to a less cooperative process. The comparison of NMR parameters of a 20-residue peptide containing two D-Pro-Gly segments (type II′ turn formers) with peptides with the negative control L-Pro-Gly led to Schenck and Gellman (1998) to assess that β-sheet formation is cooperative perpendicular to the strand direction. The existence of a positive cooperative behavior appears well-founded. However, it is equally certain that the degree of cooperativity is not too high, as inferred from the broad melting curves that are expected for peptides of this small size. The increase on the conformational H_α chemical shifts in the entire three-stranded β-sheet, as compared to those observed in components β-hairpins, is very small indeed for the peptides described (Kortemme et al., 1998; Schenck & Gellman, 1998; Sharman & Searle, 1998), which implies that the cooperativity in the formation of the β-sheet is not very large. Our 20-residue peptide 1 may show a similar index of cooperativity to that observed in the other designed peptides.

We have estimated for the first time the kinetic rate of β-sheet formation in a small model peptide. The values obtained for the β-sheet folding rate (4–14 μs at 10 °C) appear to be reasonable, if we take into account previous data on the formation of a β-hairpin (6 μs for a 16-residue peptide at room temperature (Muñoz et al., 1997)). In contrast, kinetic data for helix-coil transitions indicate that α-helix formation may be faster. Helix folding was calculated to occur in ~50 ns (Gilmanshin et al., 1997) and ~250 ns (Balew et al., 1996) from unfolding and folding studies on apomyoglobin, and in less than ~160 ns in a 21-residue peptide at 28 °C (Williams et al., 1996). Rate constants for the poly(tyrosine) coil-sheet transitions have been reported to be of the order of 100 s^{-1} (Auer & Miller-Auer, 1986). Rates of that order are shown by protein β-sheet folding as demonstrated, for example, by the formation of 90% of the native structure within 25 ms in the folding of the all-β-sheet protein Interleukin-1β (Varley et al., 1993). On the other hand, a theoretical work with a polypeptide model estimates coil-sheet rate constants of tens of ns^{-1} (Yapa et al., 1992), while another theoretical study considers that coil–β-sheet formation may be fast or slow depending on the stability of the β-sheet (Finkelstein, 1991). The lack of data concerning the formation of a pure β-sheet, and the discrepancy among the theoretical studies, may be partially solved by the future design of model β-sheet forming peptides, such as our 20-residue peptide 1, and the study of their conformational behavior.

Conclusions

We have achieved our objective of designing a linear peptide that folds into a monomeric three-stranded β-sheet. The formed β-sheet appears to be rather homogeneous since no evidence has been found of alternative conformations arising from different turn types. The success of our design demonstrates the right selection of the designing criteria: intrinsic β-sheet propensities, statistically favorable cross-strand side-chain interactions, strict dependence of

turn-type on turn residue sequence, as well as enhancement of solubility and avoidance of intermolecular interactions. The β-sheet structure formed by the designed peptide constitutes a promising model on which to investigate the factors involved in β-sheet stability. Moreover, we have been able to estimate the rate constant of the random coil-β-sheet transition. Three immediate future objectives are apparent: (1) obtaining higher β-sheet populations, (2) promoting higher levels of cooperativity, and (3) enlarging its dimensions. We believe that future designs based on this peptide system will be of great help in studying the many factors involved in β-sheet formation and stability. Advances in the understanding of the general principles governing formation of different structural motifs, in particular those containing β-structures, are expected to increase the number of successful peptide and protein designs.

Materials and methods

Peptide synthesis and purification

Peptides were synthesized by stepwise solid-phase procedures using fluorenylmethoxycarbonyl amino acids, which were activated in situ using 1H-benzotriazole-1-yl-oxy-tris-pyrrolidine-phosphonium hexafluorophosphate and N-methylmorpholine as catalyst (Coste et al., 1990). The coupling reactions were catalyzed by 1-hydroxybenzotriazole (Atherton & Sheppard, 1989). Peptides were purified by high performance liquid chromatography (HPLC) with gradients of water-acetonitrile containing 0.09% and 0.1% of trifluoroacetic acid, respectively. Peptide purity and identity were checked by HPLC and by the complete assignment of the ^{1}H-NMR spectra.

Sedimentation equilibrium

Sedimentation equilibrium experiments were performed to obtain the average molecular weight of peptide samples at 0.1 and 1 mM. Peptide samples (30 μL for 1 mM and 70 μL for 0.1 mM) were centrifuged at 40,000 rpm at 283 K in 4- and 12-mm double-sector Epon charcoal centerpieces, respectively, using a Beckman Optima XL-A ultracentrifuge with a Ti60 rotor. Radial scans were taken at different wavelengths every 2 h until equilibrium conditions were reached. The data were analyzed using the program XLAEQ from Beckman. The partial specific volume of the peptide was calculated on the basis of its amino acid composition and corrected to a temperature of 10 °C (Laue et al., 1992). The partial specific volume of the peptide is 0.717 mL/g.

NMR spectra

Peptide concentrations for NMR experiments were 1–2 mM in 0.5 mL of H_2O/D_2O (9:1 ratio by volume). The pH was measured with a glass micro-electrode and was not corrected for isotope effects. The temperature of the NMR probe was calibrated using a methanol sample. Sodium [3-trimethylsilyl 2,2,3,3-^{2}H] propionate (TSP) was used as an internal reference. The ^{1}H-NMR spectra were acquired on a Bruker AMX-600 pulse spectrometer operating at a proton frequency of 600.13 MHz. 1D spectra were acquired using 32 K data points, which were zero-filled to 64 K data points before performing the Fourier transformation. Phase-sensitive 2D correlated spectroscopy (COSY; Aue et al., 1976), total correlated spectroscopy (TOCSY; Rance, 1987), nuclear Overhauser enhancement spectroscopy (NOESY; Kumar et al., 1980), and rotating frame nuclear Overhauser effect spectroscopy (ROESY; Bothner-By et al., 1984) spectra were recorded by standard techniques using presaturation of the water signal and the time-proportional phase incrementation mode. A mixing time of 200 ms was used for NOESY and ROESY spectra. TOCSY spectra were recorded using 80 ms MLEV 17 spin-lock sequence (Bax & Davies, 1985). Additional NOESY and ROESY spectra were recorded on peptide samples in pure D_2O to facilitate the observation of the Cα*H*–Cα*H* NOE cross peaks close to the water signal. The ^{1}H-^{13}C HSQC spectra (Bodenhausen & Ruben, 1980) at natural ^{13}C abundance were recorded in 1–2 mM peptide samples in D_2O. Acquisition data matrices were defined by 2,048 × 512 points in t_2 and t_1, respectively, or 2,048 × 800, respectively. Data were processed using the standard UXNMR Bruker programs on a Silicon Graphics computer. The 2D data matrix was multiplied by a square-sine-bell window function with the corresponding shift optimized for every spectrum and zero-filled to a 2 K × 2 K complex matrix prior to Fourier transformation. Baseline correction was applied in both dimensions.

The ^{1}H-NMR spectra of peptides 1, 2, and 3 in aqueous solution were assigned using the standard sequential assignment procedure (Wüthrich et al., 1984; Wüthrich, 1986). Table 3 lists the chemical shift values of the three peptides at pH 3.4 and 10 °C. Once the ^{1}H resonances were assigned, assignment of the ^{13}C resonances was straightforward on the basis of the cross-correlations observed in the HSQC spectra between the proton and the carbon to which it is bonded. The 0 ppm ^{13}C δ was obtained indirectly by multiplying the spectrometer frequency that corresponds to 0 ppm in the ^{1}H spectrum, assigned to internal TSP reference, by 0.25144954 (Bax & Subramanian, 1986; Spera & Bax, 1991).

Structure calculation

Due to the presence of conformational averaging in linear peptides, the use of intraresidue and sequential NOEs can complicate the calculation of singular structures existing in the ensemble. For this reason only medium- and long-range NOE cross peaks were considered in the calculation of β-sheet conformation. Their intensities were used to obtain upper limit distance constraints and were evaluated qualitatively as strong (2.5 Å), intermediate between strong and medium (3 Å), medium (3.5 Å), weak (4 Å), and very weak (4.5 Å). Pseudo-atom corrections were added where necessary. The φ angles were constrained to the range −180° to 0° except for Gly and Asn. Structures were calculated on a Silicon Graphics Indigo computer using the program DIANA (Güntert et al., 1991).

Supplementary material in Electronic Appendix

Tables SM1 and SM2 list the medium- and long-range NOEs observed for peptides 2 and 3, respectively, in aqueous solution.

Acknowledgments

We thank Mrs. C. López, Mr. A. Gómez, and Mr. L. de la Vega for their technical assistance, and Drs. S. Padmanabhan, D. Laurents, L. Serrano, T. Kortemme, and M. Ramírez-Alvarado for their critical reading of the manuscript. We are grateful to Centro de Investigaciones Biológicas (CSIC) for allowing us to use the analytical ultracentrifuge. This work was supported

by the Spanish DGYCT project PB93–0189. E. de A. was the recipient of a predoctoral fellowship (AP93–51400679) from the Spanish Ministerio de Educación y Cultura.

References

Atherton E, Sheppard RC. 1989. *Solid phase peptide synthesis: A practical approach*. Oxford, UK: IRL Press.

Auer HE, Miller-Auer H. 1986. Dynamics of the disordered-β transition in poly (L-tyrosine) determined by stopped-flow spectrometry. *Biopolymers 25*:1607–1613.

Aue WP, Bertholdi E, Ernst RR. 1976. Two-dimensional spectroscopy. Application to NMR. *J Chem Phys 64*:2229–2246.

Baldwin RL. 1986. Seeding protein folding. *Trends Biochem Sci 11*:6–9.

Baldwin RL. 1995. The α-helix formation by peptides of defined sequence. *Biophys Chem 55*:127–135.

Balew RH, Sabelko J, Gruebele M. 1996. Direct observation of fast protein folding: The initial collapse of apomyoglobin. *Proc Natl Acad Sci USA 93*:5759–5764.

Bax A, Davies DG. 1985. MLEV-17-based two-dimensional homonuclear magnetization transfer spectroscopy. *J Magn Reson 65*:355–360.

Bax A, Subramanian J. 1986. Sensitivity-enhanced two-dimensional heteronuclear shift correlation NMR spectroscopy. *J Magn Res 67*:565–570.

Blanco FJ, Jiménez MA, Herranz J, Rico M, Santoro J, Nieto JL. 1993. NMR evidence of a short linear peptide that folds into a β-hairpin in aqueous solution. *Eur J Biochem 115*:5887–5888.

Blanco FJ, Jiménez MA, Pineda A, Rico M, Santoro J, Nieto JL. 1994. NMR solution structure of the isolated N-terminal fragment of protein-G B1 domain. Evidence of trifluorethanol induced native-like β-hairpin formation. *Biochemistry 33*:6004–6014.

Blanco FJ, Ramírez-Alvarado M, Serrano L. 1998. Formation and stability of β-hairpin structures in polypeptides. *Curr Opin Struct Biol 8*:107–111.

Bodenhausen G, Ruben DJ. 1980. Natural abundance nitrogen-15 NMR by enhanced heteronuclear spectroscopy. *Chem Phys Lett 69*:185–189.

Bothner-By AA, Stephens RL, Lee JM, Warren CD, Jeanloz RW. 1984. Structure determination of a tetrasaccharide: Transient nuclear Overhauser effects in the rotating frame. *J Am Chem Soc 106*:811–813.

Buckley P, Edison AS, Kemple MD, Prendergast FG. 1993. The $^{13}C_{\alpha}$-NMR assignments of melittin in methanol, and chemical shift correlations with secondary structure. *J Biomol NMR 3*:639–652.

Bundi A, Wüthrich K. 1979. The ^{1}H NMR parameters of the common amino acid residues measured in aqueous solution of linear tetrapeptides H-Gly-Gly-X-Ala-OH. *Biopolymers 18*:285–297.

Chou PY, Fasman CD. 1974. Conformational parameters for amino acids in helical, β-sheet, and random coil regions calculated from proteins. *Biochemistry 13*:211–222.

Clothia C. 1973. Conformation of twisted β-pleated sheets in proteins. *J Mol Biol 75*:295–302.

Coste J, Le-Nguyen D, Castro B. 1990. PyBOP: A new peptide coupling reagent devoid of toxic by-product. *Tetrahedron Lett 31*:205–208.

Cox JPL, Evans PA, Packman LC, Williams DH, Woolfson DN. 1993. Dissecting the structure of a partially folded protein. Circular dichroism and nuclear magnetic resonance studies of peptides from ubiquitin. *J Mol Biol 234*:483–492.

de Alba E, Blanco FJ, Jiménez MA, Rico M, Nieto JL. 1995. Interactions responsible for the β-hairpin conformation population formed by a designed linear peptide. *Eur J Biochem 233*:283–292.

de Alba E, Jiménez MA, Rico M. 1997a. Turn residue sequence determines β-hairpin conformation in designed peptides. *J Am Chem Soc 119*:175–183.

de Alba E, Jiménez MA, Rico M, Nieto JL. 1996. The ^{1}H NMR conformational investigation of designed short linear peptides able to fold into β-hairpin structures in aqueous solution. *Folding & Design 1*:133–144.

de Alba E, Rico M, Jiménez MA. 1997b. Cross-stand side-chain interactions versus turn conformation in β-hairpins. *Protein Sci 6*:2548–2560.

de Dios AC, Pearson JG, Oldfield E. 1993. Secondary and tertiary structural effects on protein NMR chemical shifts: An ab initio approach. *Science 260*:1491–1496.

Doig AJ. 1997. A three-stranded β-sheet peptide in aqueous solution containing N-methyl amino acids to prevent aggregation. *Chem Commun*:2153–2154.

Dyson HJ, Wright PE. 1993. Peptide conformation and protein folding. *Curr Opin Struct Biol 3*:60–65.

Eaton WA, Muñoz V, Thompson PA, Chan C-K, Hofrichter J. 1997. Submillisecond kinetics of protein folding. *Curr Opin Struct Biol 7*:10–14.

Finkelstein AV. 1991. Rate of β-structure formation in polypeptides. *Proteins 9*:23–27.

Freeman R. 1988a. *A handbook of nuclear magnetic resonance*. London, UK: Longman Group UK Limited. p 264.

Freeman R. 1988b. *A handbook of nuclear magnetic resonance*. London, UK: Longman Group UK Limited. p 30.

Gilmanshin R, Williams S, Callender RH, Woodruff WH, Dyer RB. 1997. Fast events in protein folding: Relaxation dynamics of secondary and tertiary structure in native apomyoglobin. *Proc Natl Acad Sci USA 94*:3709–3713.

Gronenborn AM, Clore GM. 1994. Identification of N-terminal helix capping boxes by means of ^{13}C chemical shifts. *J Biomol NMR 4*:455–458.

Guerois R, Cordier-Ochsenbein F, Baleux F, Huynh-Dinh T, Neumann J-M, Sanson A. 1998. A conformational equilibrium in a protein fragment caused by two consecutive capping boxes: ^{1}H-, ^{13}C-NMR, and mutational analysis. *Protein Sci 7*:1506–1515.

Güntert P, Braun W, Wüthrich K. 1991. Efficient computation of three-dimensional protein structures in solution from nuclear magnetic resonance data using the program DIANA, and the supporting programs CALIBA, HABAS, and GLOMSA. *J Mol Biol 217*:517–530.

Haque TS, Gellman SH. 1997. Insights on β-hairpin stability in aqueous solution from peptides with enforced type I′ and type II′ β-turns. *J Am Chem Soc 119*:3301–3302.

Hutchinson EG, Thornton JM. 1994. A revised set of potentials for β-turn formation in proteins. *Protein Sci 3*:2207–2216.

Ilyna E, Roongta V, Mayo KH. 1997. NMR structure of a de novo designed, pepide 33mer with two distinct, compact β-sheet folds. *Biochemistry 36*:5245–5250.

Kim CA, Berg JM. 1993. Thermodynamic β-sheet propensities measured using a zinc-finger host peptide. *Nature 362*:267–270.

Kortemme T, Ramírez-Alvarado M, Serrano L. 1998. Design of a 20-amino acid three-stranded β-sheet protein. *Science 281*:253–256.

Kumar A, Ernst RR, Wüthrich K. 1980. A two-dimensional nuclear Overhauser enhancement (2D NOE) experiment for the elucidation of complete proton-proton cross-relaxation networks in biological macromolecules. *Biochem Biophys Res Commun 95*:1–6.

Laue TM, Shak BD, Ridgeway TM, Pelletier SL. 1992. Computer-aided interpretation of analytical sedimentation data for proteins. In: Harding SE, Rowe AJ, Horton JC, eds. *Analytical ultracentrifugation in biochemistry and polymer science*. Cambridge, UK: Royal Society of Chemistry. pp 90–125.

Lyu PC, Wemmer DE, Zhou HX, Pinker RJ, Kallenbach NR. 1993. Capping interactions in isolated α-helices: Position-dependent substitution effects and structure of a serine-capped peptide helix. *Biochemistry 32*:421–425.

Martin F, Toniatti C, Salvati AL, Ciliberto G, Cortese R, Sollazzo M. 1996. Coupling protein design and in vitro selection strategies: Improving specificity and affinity of a designed β-protein IL-6 antagonist. *J Mol Biol 255*:86–97.

Mattos C, Petsko GA, Karplus M. 1994. Analysis of two-residue turns in proteins. *J Mol Biol 238*:733–747.

Maynard AJ, Sharman GJ, Searle MS. 1998. Origin of β-hairpin stability in solution: Structural and thermodynamic analysis of the folding of a model peptide supports hydrophobic stabilization in water. *J Am Chem Soc 120*:1996–2007.

McRorie DK, Voelker PJ. 1993. *Self-associating systems in the analytical ultracentrifuge*. Palo Alto, California: Beckman Instruments Inc.

Minor DL Jr, Kim PS. 1994a. Measurement of the β-sheet forming propensities of amino acids. *Nature 367*:660–663.

Minor DL Jr, Kim PS. 1994b. Context is a major determinant of β-sheet propensity. *Nature 371*:264–267.

Mooney EF. 1971a. *Annual reports on NMR spectroscopy*. London: Academic Press Inc. London, LTD. pp 76–77.

Mooney EF. 1971b. *Annual reports on NMR spectroscopy*. London: Academic Press Inc. London, LTD. p 84.

Muñoz V, Serrano L. 1994a. Elucidating the folding problem of helical peptides using empirical parameters. *Nature Struct Biol 1*:399–409.

Muñoz V, Serrano L. 1994b. Intrinsic secondary propensities of the amino acids, using statistical f-y matrices: Comparison with experimental scales. *Proteins Struct Funct Genet 20*:301–311.

Muñoz V, Thompson PA, Hofrichter J, Eaton WA. 1997. Folding dynamics and mechanism of β-hairpin formation. *Nature 390*:196–199.

Ralston G. 1993. *Introduction to analytical ultracentrifugation*. California: Beckman Instruments Inc.

Ramírez-Alvarado M, Blanco FJ, Niemann H, Serrano L. 1997. Role of β-turn residues in β-hairpin formation and stability in designed peptides. *J Mol Biol 273*:898–912.

Ramírez-Alvarado M, Blanco FJ, Serrano L. 1996. De novo design and structural analysis of a model β-hairpin peptide system. *Nature Struct Biol 3*:604–612.

Rance M. 1987. Improved techniques for homonuclear rotating-frame and isotropic mixing experiments. *J Magn Reson 74*:557–564.

Schenck HL, Gellman SH. 1998. Use of a designed triple-stranded antiparallel β-sheet to probe β-sheet cooperativity in aqueous solution. *J Am Chem Soc 120*:4869–4870.

Scholtz JM, Baldwin RL. 1992. The mechanism of α-helix formation by peptides. *Annu Rev Biophys Biomol Struct 21*:95–118.

Searle MS, Zerella R, Williams DH, Packman LC. 1996. Native-like β-hairpin structure in an isolated fragment from ferredoxin: NMR and CD studies of solvent effects on the N-terminal 20-residues. *Protein Eng 9*:559–565.

Sharman GJ, Searle MS. 1998. Cooperative interaction between the three strands of a designed antiparallel β-sheet. *J Am Chem Soc 120*:5291–5300.

Sibanda BL, Thornton JM. 1985. β-hairpin families in globular proteins. *Nature 316*:170–174.

Smith CK, Regan L. 1998. Construction and design of β-sheets. *Acc Chem Res 30*:153–161.

Smith CK, Withka JM, Regan L. 1994. A thermodynamics scale for the β-sheet forming tendencies of amino acids. *Biochemistry 33*:5510–5517.

Spera S, Bax A. 1991. Empirical correlation between protein backbone conformation and Cα and Cβ ^{13}C NMR chemical shifts. *J Am Chem Soc 113*:5490–5492.

Swindells MB, MacArthur MW, Thornton JM. 1995. Intrinsic φ-ψ propensities of amino acids, derived from the coil regions of known structures. *Nature Struct Biol 2*:596–603.

Varley P, Gronenborn AM, Christensen H, Wingfield PT, Pain RH, Clore GM. 1993. Kinetics of folding of the all-β sheet protein Interleukin-1β. *Science 260*:1110–1113.

Williams S, Causgrove TP, Gilmanshin R, Callender RH, Woodruff WH, Dyer RB. 1996. Fast events in protein folding: Helix melting and formation in a small peptide. *Biochemistry 35*:691–697.

Wishart DS, Bigam CG, Holm A, Hodges RS, Sykes BD. 1995. ^{1}H, ^{13}C and ^{15}N random coil NMR chemical shifts of the common amino acids. I. Investigations of nearest neighbor effects. *J Biomol NMR 5*:67–81.

Wouters MA, Curmi PM. 1995. An analysis of side-chain interactions and pair correlations within antiparallel β-sheets: The differences between backbone hydrogen bonded and nonhydrogen bonded residue pairs. *Proteins 22*:119–131.

Wright PE, Dyson HJ, Lerner RA. 1988. Conformation of peptide fragments of proteins in aqueous solution: Implication for initiation of protein folding. *Biochemistry 27*:7167–7175.

Wüthrich K. 1986. *NMR of proteins and nucleic acids*. New York: J. Wiley & Sons.

Wüthrich K, Billeter M, Braun W. 1984. Polypeptide secondary structure determination by nuclear magnetic resonance observation of short proton-proton distances. *J Mol Biol 180*:715–740.

Yao J, Dyson HJ, Wright PE. 1997. Chemical shift dispersion and secondary structure prediction in unfolded and partly folded proteins. *FEBS Lett 419*:285–289.

Yapa K, Weaver DL, Karplus M. 1992. β-sheet coil transitions in a simple polypeptide model. *Proteins 12*:237–265.

Yibing Y, Erickson BW. 1994. Engineering of Betabellin 14D: Disulfide-induced folding of a β-sheet. *Protein Sci 3*:1069–1073.

Zhou NE, Kay CM, Sykes BD, Hodges RS. 1993. A single-stranded amphipathic α-helix in aqueous solution: Design, structural characterization, and its application for determining α-helical propensities of amino acids. *Biochemistry 32*:6190–6197.